KAWASAKI STEEL TECHNICAL REPORT
No.24 (April 1991)

Development of Coiling Temperature Control System on Hot Strip Mill

Kazuhiro Yahiro, Jujiro Yamasaki, Masahiro Furukawa, Kazuo Arai, Masahiko Morita, Masamitsu Obashi

Synopsis :
At the Mizushima Works hot strip mill, a newly developed cooling control system has been introduced downstream of the finishing mill as a means of improving product quality uniformity. The system includes a transformation progress model tuned by an on-line transformation detector and a precise temperature model in which consideration is given to the dependence of the heat transfer coefficient on temperature and temperature distribution in the depth direction. The two models make possible the exact prediction of changes in surface and mean temperatures, and of the transformed fraction in the cooling process, resulting in improved coiling temperature accuracy and better product uniformity.

The body can be viewed from the next page.

Development of Coiling Temperature Control System on Hot Strip Mill*


Kazuhiro Yahiro
Staff Assistant Manager, Plant Control Technology Sec., Mizushima Works


Jujiro Yamasaki
Staff Assistant General Manager, Plant Control Technology Sec., Mizushima Works


Masahiro Furukawa
Hot Rolling Technology Sec., Mizushima Works


Kazuo Arai
Senior Researcher, Mechanical Processing, Instrumentation and Control Research Center, I & S Res. Labs.


Masahiko Morita
Senior Researcher, Sheet Lab., I & S Res. Labs.


Masamitsu Obashi
Staff Manager, Energy Technology Sec., Mizushima Works

Synopsis:

At the Mizushima Works hot strip mill, a newly developed cooling control system has been introduced downstream of the finishing mill as a means of improving product quality uniformity. The system includes a transformation progress model tuned by an on-line transformation detector and a precise temperature model in which consideration is given to the dependence of the heat transfer coefficient on temperature and temperature distribution in the depth direction. The two models make possible the exact prediction of changes in surface and mean temperatures, and of the transformed fraction in the cooling process, resulting in improved coiling temperature accuracy and better product uniformity.

1 Introduction

In hot strip mills, strip is cooled as it passes over a runout table located downstream of the finishing stands, then coiled at a specified temperature known as the coiling temperature. Because control of the cooling process is essential in determining the mechanical properties of the material, computer-based coiling temperature control systems were introduced at an early date.

At Mizushima Works hot strip mill, a computerized coiling temperature control system was introduced in 1977, and has contributed significantly to the enhancement of product quality.[1] The expanded control range required by the recent diversification of product types as well as user needs for better uniformity of product quality have made a higher level of control accuracy and improved product quality indispensible. Further, the heat transfer and metallurgical phenomena associated with the cooling process are complex, and as such have generally been considered uncontrollable factors limiting the control accuracy of conventional systems.

For these reasons, the coiling temperature control system at Mizushima Works was completely redesigned with the aim of expanding its range of functions and upgrading its accuracy. Essential points in the realization of the new system were the development of a model capable of reproducing heat transfer and metallurgical phenomena and adaptive control technology adequate to cope with process changes.

This report presents an outline of the new coiling temperature control system, focusing on its three principal functions, and briefly describes the results of its introduction. The control models on which the temperature control system is based are discussed in detail.

2 General Description of Equipment

The layout of the cooling facilities at the Mizushima hot strip mill is shown in **Fig. 1**; the specifications of the equipment are given in **Table 1**. To allow precise control of the cooling process at the run-out table, the

* Originally published in *Kawasaki Steel Giho*, 22(1990)1, pp. 12–18

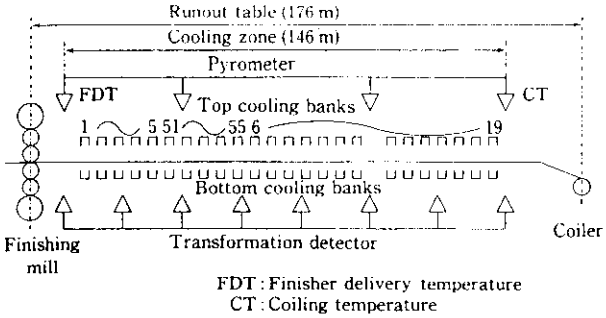

Fig. 1 General layout of strip cooling devices on runout table

Table 1 Specifications of cooling device at runout table

Spray form	Top	No. 1~19	Pipe laminar
		No. 51~55	Slit laminar
	Bottom		Flat spray
Number of cooling control units	Top	No. 1~19	63
		No. 51~55	16
	Bottom		50
Pumping capacity			282 m³/min
Cooling tower capacity			35 m³/min, 45°C→32°C
Number of cooling control zone			24

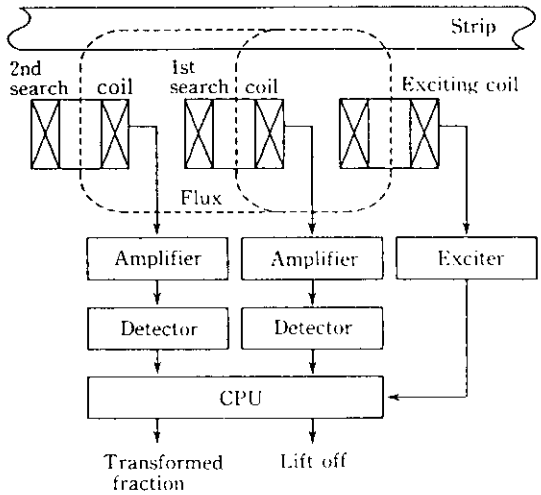

Fig. 2 Block diagram of the sensor for transformation measurement

cooling banks of the water cooling system are divided into 24 cooling zones, with each bank containing a number of control units (three-way valves). In the upper cooling banks, Nos.1-19 are of the pipe-laminar type, while Nos.51-55 are of the slit-laminar type, which provides high capacity cooling with excellent transverse uniformity.[2] Banks No.1-4 are provided with a water flow rate control function.

The run-out table is equipped with eight transformation detectors, each including an exciter coil and two search coils. The operational principle of the magnetic induction method used in the detection devices is shown in **Fig. 2**.[3] This method is based on the phenomenon that the changes in the voltage present in the search coils when an ac magnetic flux is generated by the exciter coil correspond to changes in the relative magnetic permeability and electric conductivity associated with the γ/α transformation in the magnetic domain present in the steel under measurement. The use of two search coils makes it possible to measure and compensate for the distance between the sensor and the hot strip on the basis of differences in the distance dependence of the two coils.

3 New Coiling Temperature Control System

3.1 Concept of System Development

The cooling behavior of strip passing over the run-out table depends on both physical phenomena related to the iterior of the material and external phenomena. Internal factors include conduction of heat in the thickness direction and phase-transformation heat generation, as well as changes in physical values (specific heat, thermal conductivity) brought about by changes in phase distribution (α phase, γ phase) and temperature. External factors include conductive cooling during water cooling and radiant and convective cooling during air cooling.

To achieve precise control of cooling, it is necessary to obtain as accurate an understanding as possible of the heat transfer related to each of the above-mentioned physical phenomena, and on this basis to determine the appropriate degree of cooling. Although certain of these factors were included in conventional coiling temperature control systems either by means of tabulation or regressive formulas, the newly developed system gives more rigorous consideration to these phenomena with the aim of absolute minimization of variations in temperature control performance.

The major differences between the old and new coiling temperature control systems are compared in **Table 2**. While one aim of the new system was to improve the accuracy of coiling temperature control, the following were also considered important in the system design from the practical viewpoint of realizing a comprehensive, high-accuracy control system for strip cooling on the run-out table:

(1) To obtain an accurate grasp of cooling behavior at each of the runout table control bank positions, not only coiling temperature but also the temperature and transformed fraction at each control bank are measured.

Table 2 Comparison between new and conventional coiling temperature control systems

Terms	New system	Conventional system
Dependence of heat transfer coefficient on temperature	Considered	Neglected
Radiation of latent heat of transformation	Considered	Neglected
Calculation of temperature	All section at runout table	Only FDT and CT
Temperature distribution in depth direction	Considered	Neglected

(2) To improve the accuracy of temperature prediction, temperature models were developed and introduced with consideration given to the temperature dependence of the heat transfer coefficient, transformation progress and transformation heat generation of the strip, and temperature distribution in the thickness direction.

(3) To obtain an exact understanding of changes in the capacity of the water cooling banks over time, a complex learning formula for water cooling bank capacity was developed using the method of recursive least squares.

3.2 Configuration of System Functions

The system configuratin of the coiling temperature control system is shown in **Fig. 3**. The central computer (C/C) is responsible for control of the production plan and results, while the on-line computer (O/C) provides operational support. The process computer (P/C) level comprises SCC1 and SCC2 (supervisory control computers 1 and 2), and FEP2 (front end processor 2). SCC1 serves as a general computer, relaying coiling

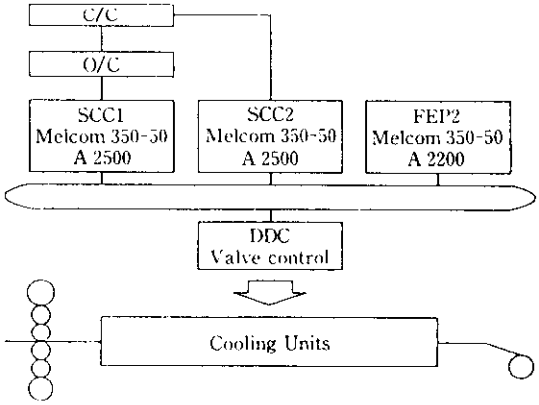

Fig. 3 System configuration of the cooling control system

temperature commands to FEP2. On the other hand, SCC;, which is responsible for quality control, receives process results from FEP2 and transmits them to the C/C. Based on the coiling temperature instructions of SCC1, FEP2 makes the necessary cooling calculations for the entire process from the delivery side of the finishing mill through the completion of coiling and controls the cooling capacity of the line accordingly. FEP2 also collects data for quality control and analysis.

The configuration of coiling temperature control functions performed by FEP2 is shown in **Fig. 4**. This system is comprised of the following four main functions:

(1) Temperature Calculation

Using a temperature model which combines analytic solution by a non-steady one-dimensional heat conduction equation with a model for transformation progress and heat generation, predictive calculations are made for the temperature and transformed fraction at each control section. These

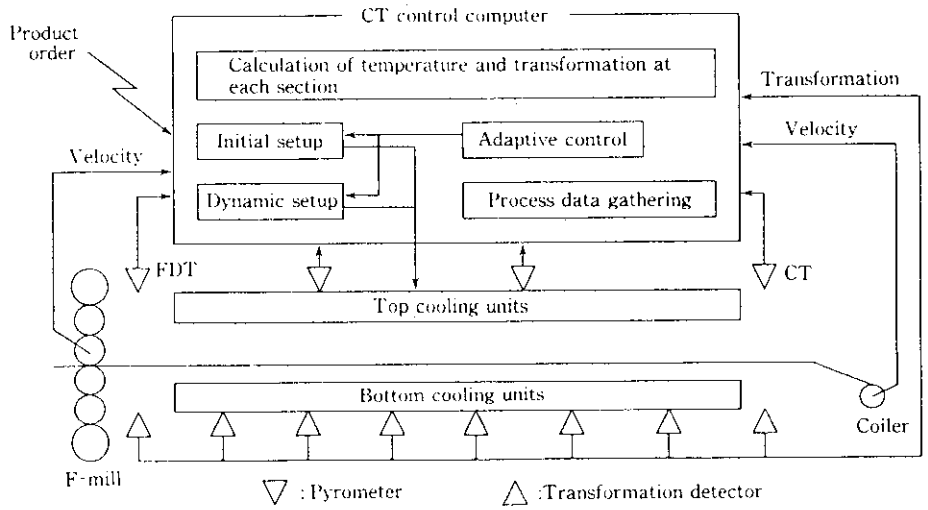

Fig. 4 Conceptional diagram of cooling control

calculations are reflected in the cooling control system in dynamic setting calculations as well as in learning calculations.

(2) Initial Setup
In order to satisfy the cooling conditions applied to respective strips, the necessary degree of cooling for the lead end of the strip is obtained using the temperature model. This value is used as the initial setting for the cooling section. Setup of the initial value is executed as the strip enters the finishing train.

(3) Dynamic Setup
The necessary cooling at specified intervals along the moving strip is obtained using the temperature model, with consideration given to changes in FDT and speed. The values obtained are used in dynamic control of the cooling facilities.

(4) Adaptive Control
The recursive least square method is applied to the coiling temperature calculated by the model on the basis of actual cooling performance and to the coiling temperature as measured by a pyrometer. The learning function provides a more accurate grasp of the effect of air cooling and the real capacity of the cooling banks.

3.3 Method of Coiling Temperature Control

In the coiling temperature control system, a target cooling pattern such as that shown in **Fig. 5** is received from the higher order computer. Using this information, target entry and exit side temperatures are obtained for each zone, and required cooling water quantity is calculated using the method illustrated in **Fig. 6**, which shows the outline of the algorithm used in calculating initial setup and dynamic setup values. The number of units of water cooling required to satisfy the cooling conditions applied is estimated and a temperature calculation is made using the temperature model; a calculated coiling temperature is then obtained. When determining the number of units of cooling water required, the number of units of cooling water is increased until the difference between the calculated coiling temperature and the value applied to the cooling line is smaller than a constant ε.

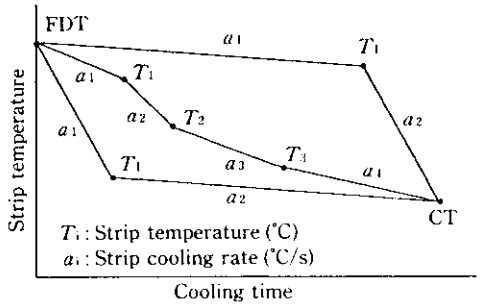

Fig. 5 Strip cooling patterns on runout table

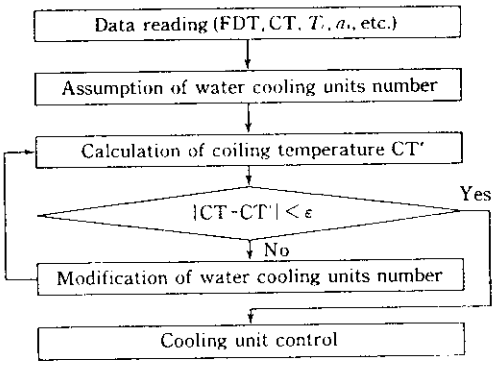

Fig. 6 Flow diagram of set-up calculation for cooling units

3.4 Control Models

3.4.1 Strip Temperature Change Model

In the strip temperature change model, it is necessary to be able to measure the strip temperature in real time and further, to be able to calculate a mean temperature for use in predicting transformation phenomena and surface temperature in order to make an appropriate estimate of the rate of heat transfer during cooling. Generally, the internal temperature distribution of steel strip is as represented by the following equations:[4]

$$c\rho\frac{\partial T}{\partial t} = \frac{\partial}{\partial x}\left(k\frac{\partial T}{\partial x}\right) + H \quad \cdots\cdots\cdots\cdots\cdots\cdots (1)$$

surface: $-k(\partial T/\partial x) = \alpha(T - T_L)$

center: $-k(\partial T/\partial x) = 0$

where c: Specific heat (kcal/kg°C)
ρ: Density (kg/m^3)
T: Temperature of steel strip (°C)
t: Cooling time (h)
x: Position in material (m)
k: Thermal conductivity (kcal/m · h°C)
H: Latent heat rate of phase transformation (kcal/m^3 · h)
α: Heat transfer coefficient (kcal/m^2 · h °C)
T_L: Temperature of cooling medium (°C)

The authors adopted the analytic solution of non-steady one-dimensional heat conduction equation (Eq. (1)) as a high-precision on-line temperature model. Conventionally, however, this analytic solution was difficult to apply to on-line real-time operation because, although it was possible to calculate the temperature distribution in the thickness direction, a progressive formula was used, while on the other hand a convergent calculation was necessary to obtain parameters. An attempt was therefore made to express the analytic solution in an algebraic form which would in no way

involve calculation of the sum of a series or convergent calculation. It was thus possible to express mean temperature using the following equation[5]:

$$\bar{T}' = (\bar{T} - T_L)\exp\left\{-\frac{4a}{d^2}\cdot X_1^2\cdot t\right\} + T_L \quad \cdots\cdot(2)$$

where $\bar{T}, \bar{T}'$: Mean temperature of strip before and after cooling (°C)
d: Strip thickness (m)
a: Heat transmission ratio (m^2h)

Parameter X_1 is given as the root of the following transcendental equation:

$$B_1 = 2X_1 \tan X_1 \cdots\cdots\cdots\cdots\cdots\cdots\cdots\cdots(3)$$

B_i: Biot's number $(= \alpha \cdot d/k)$

The following equation was derived as an algebraic expression of Eq.(3):

$$\left.\begin{aligned} X_1 &= \{p[1 - \sqrt{1 - 15B_i/(2Mp^2)}\,]\}^{1/2} \\ p &= \{B_i(M + 5) + 30\}/4M \\ M &= f(B_i) \end{aligned}\right\} \cdots\cdots(4)$$

After calculation of the mean temperature, the surface temperature is calculated using a formula for the average temperature position and a conversion formula for the ratio of internal to surface temperaure. Finally, the internal temperature distribution is calculated.

In deriving a relation for the average temperature position, Eq. (5) defines the neutral point of heat values as equal to the mean temperature position, while Eq. (6), which gives the ratio of internal temperature to surface temperature, is based on the principle of conservation of thermal energy and Fourier's Law.[5]

$$\left.\begin{aligned} \bar{\beta} &= (1 + A^{-1})\left\{1 - \sqrt{\frac{0.5 + A^{-1}}{(1 + A^{-1})^2}}\right\} \\ A &= B_i(1 - T_L/T_S)/2 \\ \bar{\beta} &= 2\bar{x}/d \end{aligned}\right\} \cdots\cdots(5)$$

$$T_B/T_S = 1 + A(1 - \beta) \cdots\cdots\cdots\cdots\cdots\cdots(6)$$

where $\bar{x}$: Mean temperature position (m)
$\bar{\beta}$: Coefficient of mean temperature position
T_S: Surface temperature of steel strip (°C)
T_B: Internal temperature of steel strip (°C)
β: Coefficient of internal position

However, in a transitional period, which is in the initial stage of cooling when the temperature at the center of the material has not yet shown any decrease, another formula is applicable for internal temperature distribution.

When the calculations made using the algebraically expressed temperature model derived from Eqs.(2) and (4) to (6) were subjected to differential calculation and a comparison was made for a wide range of conditions (strip thickness, 1–32 mm; heat transfer coefficient, 75–750 kcal/m^2 · h°C; cooling time, 0.5–30 s), only a slight deviation of 0–2°C was found. This level of precision was considered satisfactory for practical application.

3.4.2 Water cooling heat transfer coefficient model

The capacity of the water cooling nozzles is determined by a variety of factors. In this model, the following factors are included in calculations of the water cooling heat transfer coefficient:

(1) Surface temperature of steel strip
(2) Nozzle configuration (pipe laminar, slit laminar, spray)
(3) Water volume density
(4) Water temperature

The heat transfer coefficient which is used in calculating the Biot's number in Eq.(3) may be expressed by Eq.(7).

$$\alpha = A + B\exp[C\cdot(T_S - D)^2 \cdots\cdots\cdots\cdots(7)$$

A, B, C, and D: Coefficients

The heat transfer coefficients calculated with the above equation, however, are revised by taking the heat transfer coefficient of the pipe laminar section as a standard and using relative coefficients for the other types of nozzles, water volume density, and water temperature.[6]

3.4.3 Air cooling heat transfer coefficient model

Among the factors contributing to air cooling of the strip as it passes over the run-out table are radiant convective heat transfer and conductive cooling caused by contact with the run-out table rolls. Conventionally, Stephan-Bolzmann's Law, which is shown in Eq.(8), has been applied to radiant heat transfer.[7]

$$q_{rad} = \varepsilon\sigma[(T_S + 273)^4 - (T_{air} + 273)^4] \cdots\cdot(8)$$

where T_{air}: Air temperature (°C)
σ: Stephan-Bolzmann's constant (kcal/m^2 · h · k^4)
ε: Rate of radiation
q_{rad}: Heat flux by radiation (kcal/m^2 · h)

Newton's law of cooling is applied to convective heat transfer and heat conduction to the run-out table rolls.[7]

$$q_{conv} = \alpha_{conv}(T_S - T_{air}) \cdots\cdots\cdots\cdots\cdots(9)$$

α_{conv}: Coefficient of convective heat transfer (kcal/m^2 · h · °C)
q_{conv}: Heat flux by convection (kcal/m^2 · h)

The value of thermal transfer coefficient in air cooling, as used in Eq.(3), can be expressed by the following equation:

$$\begin{aligned} \alpha &= (q_{rad} + q_{conv})/(T_S - T_{air}) \\ &= \varepsilon\sigma\{(T_S + 273)^4 - (T_{air} + 273)^4\}/(T_S - T_{air}) + \alpha_{conv} \end{aligned} \quad \cdots\cdots\cdot(10)$$

In order to use Eq.(10) as a model for on-line application, the values of ε and α_{conv} must be known. For ε,

values of 0.6–0.85 were obtained on the basis of measurements taken using a short wavelength (3.8 μm) pyrometer,[8] while α_{conv} values were in the natural range for convective turbulence at 7 to 15 kcal/m^2 · h · °C.[9,10] Further, the heat transfer coefficient related to conductive heat transfer from the strip to the rolls cannot be ignored when determining α_{conv}. For this reason, α is obtained from measured results for rolling without water cooling, and the ε and α_{conv} which are necessary to satisfy this value are obtained from Eq.(10).

3.4.4 Model for rate of phase transformation

Well known equations for static recrystallization in steel have been proposed by Johnson and Mehl[11] and Avrami[12]. If X is taken as the rate of phase transformation and recrystallization nuclei are presumed to be generated uniformly at generation rate I_h and then to grow in spherical form at growth speed G, the rate of phase transformation can be expressed by Eq.(11):

$$X = 1 - \exp\left(-\frac{\pi}{3} I_h G^3 t^4\right) \cdots\cdots\cdots\cdots (11)$$

In this equation, I and G are factors affected by the chemical composition of the steel, the austenite grain size after finishing rolling, and the distortion energy within the austenite grains, as well as by transformation temperature and the passage of time. Thus, Eq.(11) can be shortened as follows:

$$X = 1 - \exp(-kt^n) \cdots\cdots\cdots\cdots (12)$$

Here, k and n are constants determined by chemical composition and the kinetic conditions affecting the austenite grains. Although a model clarifying the physical significance of these factors would be necessary for a precise description of recrystallization, research in this area[13] is still only in the early stages. The concept used in constructing a model of recrystallization in this report is fundamentally based on Eq.(12), with priority given to the speed of calculation in practical circumstances from the viewpoint of on-line application. For this reason, the values of k and n in the model discussed here were obtained by statistical methods from simple, practical measured data. The basic equation for recrystallization in this report is shown below as Eq. (13):

$$X = 1 - \exp[-K(t/t_{50})^n] \cdots\cdots\cdots\cdots (13)$$

The symbol t_{50} indicates the time from the exit of the finishing train until a transformation ratio of 50% has been achieved. Thus, Eq.(13) uses the point t_{50} to indicate the time at which the $\gamma \longrightarrow \alpha$ transformation is 50% complete and corresponds to the Johnson-Mehl-Avrami equation, which uses a value of n as an index value.

As mentioned previously, t_{50} and n in Eq.(13) are parameters which affect transformation characteristics related to chemical composition and the kinetic conditions affecting the austenite grains. In order to establish these parameters, an on-line transformation detector developed by the authors was installed at eight points on the run-out table and statistical processing was applied to the measured results of the transformed fraction, chemical composition, and hot rolling data obtained with commercially rolled material.

3.4.5 Transformation latent heat model

In ferrite-pearlite (F-P) phase steels, if the F phase ratio X_F and the transformation latent heat for γ (austenite) $\longrightarrow$ F, q_F, and for $\gamma \longrightarrow$ P, q_P, are known, then $\gamma \longrightarrow$ F + P transformation latent heat q_T can generally be obtained using Eq. (14).

$$q_T = X_F q_F + (1 - X_F) q_P \cdots\cdots\cdots\cdots (14)$$

In this equation, X_F can be calculated if the carbon content, C, eutectoid carbon content, C_e, and the solid solution limit for carbon in the F phase C_F are known. Ignoring the change in C_F brought about by addition of the alloying element Y_i, if C_e is expressed as a formula using the data shown in **Fig. 7**,[14] X_F can be obtained from Eq. (15).

$$X_F = (C_e - C)/(C_e - C_F) \cdots\cdots\cdots\cdots (15)$$

$$C_F \leq C \leq C_e$$

$$C_e = C_e^* + \sum_{i=1}^{n} (a_i A_{Y_i}^3 + b_i A_{Y_i}^2 + c_i A_{Y_i})$$

Here, C_e^* is the eutectoid carbon content ratio of the Fe-C binary alloy, A_{Y_i} is the added content of the alloying element Y_i, and C_F, a_i, b_i, and c_i are given coefficients.

In the same manner, the $\gamma \longrightarrow$ F transformation latent heat, q_F, can be obtained from Eq. (16):

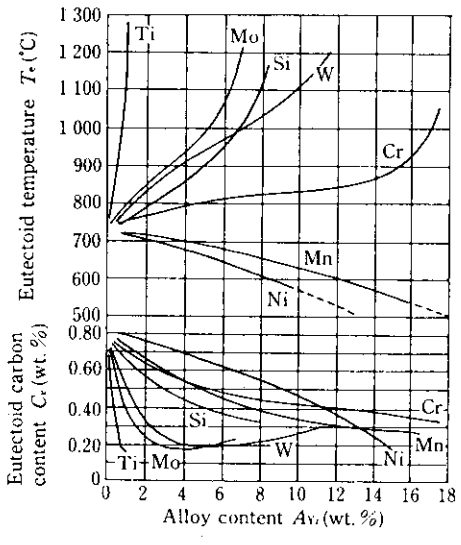

Fig. 7 Influence of alloy content on eutectoid temperature and carbon content[14]

$$q_F = q_F^* + \sum_{i=1}^{n} (d_i A_{Y_i}^3 + e_i A_{Y_i}^2 + f_i A_{Y_i}) \cdots (16)$$

In Eq.(16), q_F^*, d_i, e_i, and f_i are obtained as coefficients from the documentary data in Fig. 7.[14] The $\gamma \longrightarrow$ P transformation latent heat, q_P, can be expressed by Eq. (17) if the volmetric ratio of F_3C in P, $X_{P/C}$, and $\gamma \longrightarrow Fe_3C$ transformation latent heat, q_C^*, are known.

$$q_P = q_C^* X_{P/C} + (1 - X_{P/C}) q_F \cdots (17)$$

Values for use in the control system are established by obtaining fundamental transformation latent heat amounts from Eqs.(14)-(17) and correcting for deviation from the measured data.

3.4.6 Adaptive control model

With the aim of correcting the error which occurs over time in the cooling equipment, the adaptive control model compares the values calculated in accordance with the models against measured values and applies the results to the following and subsequent coils. Two methods of adaptive control are apossible, one in which the deviations resulting from control practices are applied as a unit to a single representative cause of error, and the other in which deviations are categorized by cause. In the first case, because various causes of error are represented by a single learning coefficient, the learning coefficient cannot be stabilized. For this reason, the latter, multi-factor learning method was adopted.

In this system, causes of deviation are categorized by each water cooling bank as part of the learning function. The temperature drop at the run-out table is expressed as follows:

$$\mathrm{FDT} - \mathrm{CT} = \sum_{i=1}^{N} C_{W_i} \cdot \Delta T_{W_i} + C_a \sum_{i=1}^{N} \Delta T_{a_i} \cdots (18)$$

where C_{W_i}: Learning coefficient for water cooling at bank i

C_a: Learning coefficient for air cooling

ΔT_{W_i}: Temperature drop caused by water cooling at bank i

ΔT_{a_i}: Temperature drop caused by air cooling at bank i

Equation (16) can thus be rewritten as follows:

$$\left.\begin{aligned} Y_t &= \boldsymbol{\Phi}_t^T \boldsymbol{\theta}_t \\ Y_t &= [\mathrm{FDT} - \mathrm{CT}]_t \\ \boldsymbol{\Phi}_t &= [\Delta T_{W_1}, \Delta T_{W_2}, \ldots, \Delta T_{W_N}, \sum_{i=1}^{N} \Delta T_{a_i}]_t^T \\ \boldsymbol{\theta}_t &= [C_{W_1}, C_{W_2}, \ldots, C_{W_N}, C_a]_t^T \end{aligned}\right\} \cdots (19)$$

The subscript t indicates data taken at sampling point t, while the superscript T indicates the transposed matrix. The symbols FDT and CT are defined by measured temperature values.

If the method of recursive least squares[15] is applied to Eq.(19), he learning coefficient $\hat{\boldsymbol{\theta}}_t$ as given by the following equation becomes identical with on-line conditions.

$$\left.\begin{aligned} \hat{\boldsymbol{\theta}}_t &= \hat{\boldsymbol{\theta}}_{t-1} + \boldsymbol{\Gamma}_t (Y_t - \boldsymbol{\Phi}_t^T \hat{\boldsymbol{\theta}}_{t-1}) \\ \boldsymbol{\Gamma}_t &= \boldsymbol{P}_{t-1} \boldsymbol{\Phi}_t / (1 + \boldsymbol{\Phi}_t^T \boldsymbol{P}_{t-1} \boldsymbol{\Phi}_t) \\ \boldsymbol{P}_t &= \boldsymbol{P}_{t-1} - \boldsymbol{P}_{t-1} \boldsymbol{\Phi}_t (1 + \boldsymbol{\Phi}_t^T \boldsymbol{P}_{t-1} \boldsymbol{\Phi}_t)^{-1} \boldsymbol{\Phi}_t^T \boldsymbol{P}_{t-1} \end{aligned}\right\} \cdots (20)$$

By using the learning coefficients obtained from Eq. (20) to correct the capacity coefficients of the individual cooling banks given in Eq.(18), continuing improvement of the accuracy of the models can be achieved. For other causes of error, data is collected on-line as necessary and used in the correction of values.

4 Evaluation of System

4.1 Evaluation of Control Models

The accuracy of the temperature model under operational conditions is shown in **Fig. 8**, which gives a com-

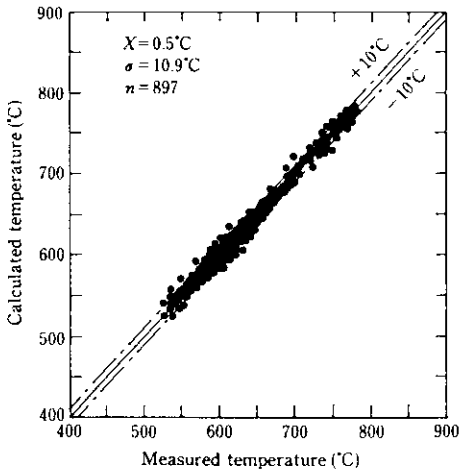

Fig. 8 Relation between measured coiling temperature and calculated coiling temperature

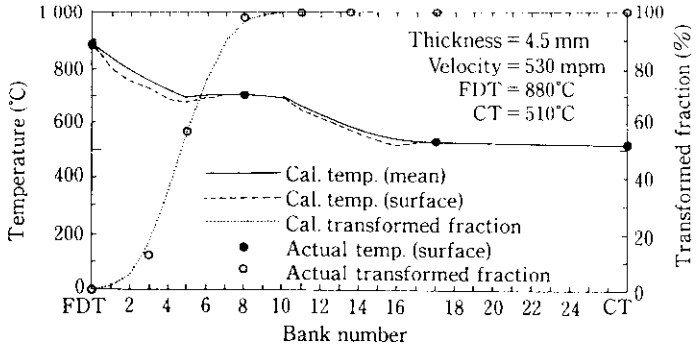

Fig. 9 Example of process model calculation of cooling zone

parison of calculated and measured temperatures. The standard deviation was $1\sigma = 10.9$°C. The example of a process model temperature calculation in **Fig. 9** shows the progress of changes in strip temperature and the rate of transformation in response to water and air cooling. The measured results show good agreement with the calculated values. Using a model combining the respective models dicussed in Sec. 3.4, it is possible to predict strip surface temperature, average temperature, and changes in the rate of transformation duing the cooling process with a high degree of accuracy.

4.2 Evaluation of Control Results

Results of the application of the new coiling temperature control system to commercial equipment as shown in **Figs. 10** and **11**. The comparison of the coiling temperature control results using the old and new systems in Fig. 10 shows a marked improvement in coil-by-coil uniformity following adoption of the new model. Figure 11 shows changes in the accuracy of coiling temperature as measured by the percentage of coil length which falls within ±20°C of the target coiling temperature. With the introduction of the new system, this measure of coiling temperature accuracy has improved from 90.0% to 97.8%.

4.3 Evaluation of Product Quality

An example of product quality improvement with the new system is shown in **Fig. 12** for a 0.15% C-0.75% Mn steel, indexed to variations in mechanical

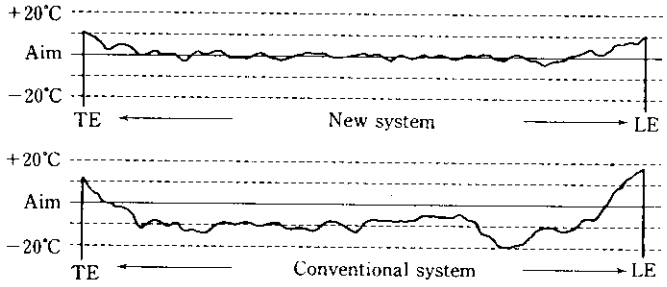

Fig. 10 Example of coiling temperature control (thickness = 2.5 mm)

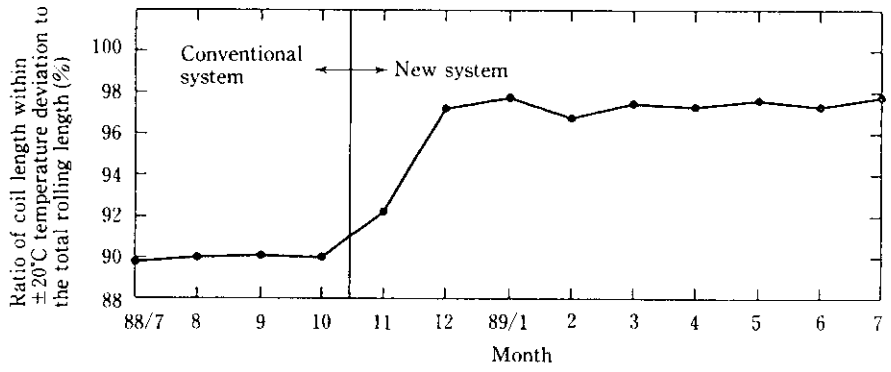

Fig. 11 Accuracy of coiling temperature

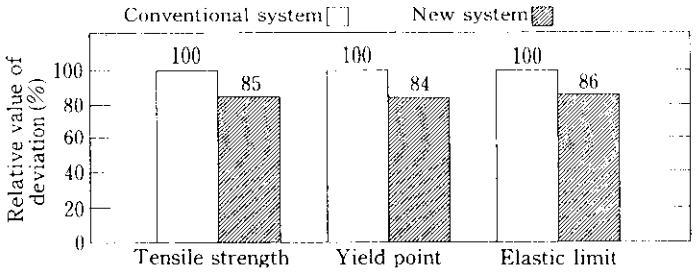

Fig. 12 Improvement of accuracy of mechanical properties (0.15% C–0.75% Mn steel)

properties prior to introduction (i.e., the index 100 represents mechanical property deviations using the conventional system). Variations in tensile strength (TS), yield point (YP), and elongation (El) were all reduced by approximately 15%, indicating that significant improvement in the uniformity of mechanical properties can be achieved with the new cooling control system.

5 Conclusions

With the aim of improving product quality at Mizushima Works hot strip mill, the cooling control system downstream of the finishing mill was renovated. The new system has been in commercial operation since November 1988. Features of the system are described below.

(1) The existing model equations used in cooling were reviewed and a model temperature equation was developed, with consideration given to temperature distribution in the strip thickness direction, the temperature dependent characteristics of the heat transfer coefficient, transformation progress, and latent heat of transformation.

(2) The newly developed temperature model was applied to cooling control, and a predictive accuracy of $1\sigma = 10.9°C$ was achieved for coiling temperature.

(3) The temperature calculation model has been applied not only to coiling temperature, but also to individual control of the cooling sections, providing highly accurate control of strip cooling behavior.

(4) Application of the method of recursive least squares makes it possible to apply a learning function to the cooling capacity of each of the cooling banks and to quantify changes in cooling bank capacity over time.

(5) A 7.8% improvement in the $\pm 20°C$ coiling temperature hit rate (relative to the length of the individual strip) has been achieved. Further, variations in each of several important product quality indicators, including TS, YP, and El, have been reduced by approximately 15%.

This newly developed cooling control system for the hot strip mill combines a high degree of consistency with extremely precise control of coiling temperature, and has resulted in significantly improved product quality and a reduction in manpower requirements.

References

1) Y. Miyake, T. Niside, S. Moriya, T. Ikenaga, T. Inoue, and K. Takagi: *Kawasaki Steel Giho*, **10**(1978)1, 58–69
2) M. Miyaguchi, T. Inoue, K. Hamada, M. Kanome, T. Naoi, and S. Nakano: *Tetsu-to-Hagané*, **72**(1986)4, S338
3) M. Morita, K. Hashiguchi, S. Okano, O. Hashimoto, and M. Nishida: *Tetsu-to-Hagané*, 71(1985)13, S1089
4) W. H. Giedt: "Principles of Engineering Heat Transfer" [D. Van Nostrand Co.]
5) K. Arai: *Tetsu-to-Hagané*, 72(1987)5, S384
6) Private communication
7) J. P. Holman: "HEAT TRANSFER", [McGraw-Hill]
8) Y. Fukutaka and T. Iwamura: *CAMP-ISIJ*, **1**(1988), 1587
9) J. Komon: *Sosei-to-Kakou (J. Jap. Soc. Tech. of Plasticity)*, 11(1970)118, 816–824
10) Private communication
11) M. A. Johnson and R. F. Mehl: *Trans. AIME*, **135**(1939), 416
12) M. Avrami: *J. Chem. Phys*, **7**(1939), 1103
13) M. Umemoto and I. Tamura: *CAMP-ISIJ*, **2**(1989), 3688
14) E. C. Bain: "Function of Alloying Element in Steel", ASM, (1940)
15) S. Sagara, A. Akizuki, T. Nakamizo and T. Katayama: "System-Doutei", 116–118 [The Soc. of Instrument and Controll Engineers]